

1N-31

152274

## Design optimization and analysis of a composite honeycomb intertank

Jeffrey Finckenor

*National Aeronautics and Space Administration, Marshall Space Flight Center, ED52, Huntsville, AL 35812, USA*

### Abstract

Intertanks, the structure between tanks of launch vehicles, are prime candidates for weight reduction of rockets. This paper discusses the optimization and detailed analysis of a 96" (2.44 m) diameter, 77" (1.85 m) tall intertank. The structure has composite face sheets and an aluminum honeycomb core. The ends taper to a thick built up laminate for a double lap bolted shear joint. It is made in 8 full length panels joined with bonded double lap joints. The nominal load is 4000 lb/in ( $7 \cdot 10^5$  N/m).

Optimization is by Genetic Algorithm and minimizes weight by varying core thickness, number and orientation of areage and buildup plies, and the size, number and spacing of bolts. A variety of cases were run with populations up to 2000 and chromosomes as long as 150 bits. Constraints were buckling, face stresses (normal, shear, wrinkling and dimpling), bolt stress, and bolt hole stresses (bearing, net tension, wedge splitting, shear out and tension/shear out). Analysis is by a combination of theoretical solutions and empirical data.

After optimization, a series of coupon tests were performed in conjunction with a rigorous analysis involving a variety of finite element models. The analysis and test resulted in several small changes to the optimized design.

The intertank has undergone a 250,000 lb ( $1.1 \cdot 10^6$  N) limit load test and been mated with a composite liquid hydrogen tank. The tank/intertank unit is being installed in a test stand where it will see 200 thermal/load cycles. Afterwards the intertank will be demated and loaded in compression to failure.

## Introduction

The composite intertank was designed and built by NASA/Marshall Space Flight Center as part of phase I of X-33 prior to selecting a single contractor. Phase I work was intended to prove technologies which would be required for the X-33 and eventually a Reusable Launch Vehicle. The intertank is part of the Composite Primary Structure task and was done in conjunction with a composite liquid hydrogen (LH2) tank made by Boeing North American (then Rockwell International) as part of the Cryogenic Tankage task. The intertank and tank are to be tested as a unit to provide information not only on the components themselves, but on a major structural composite joint in a relevant environment.

The Rockwell X-33 proposal was for a wing-body vehicle, while Lockheed-Martin proposed a lifting body and McDonnell Douglas (now Boeing) proposed a conical vertical take-off, vertical landing vehicle. The tank and intertank are 8' (2.44 m) diameter subscale components of the proposed 30' (9.14 m) diameter wing-body vehicle. The focus was on the Rockwell wing-body, but was applicable to any of the vehicles, as indicated in Figure 1. The prime technology demonstrations of the intertank are oven curing and bonded assembly of large composite structures.

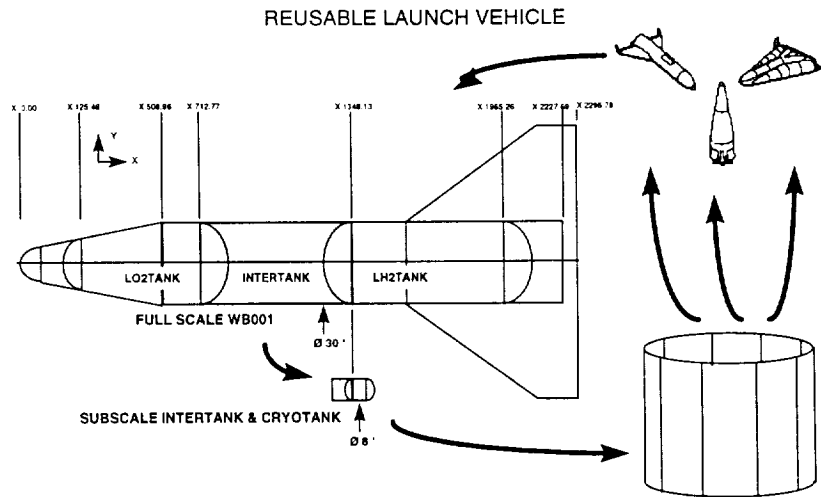


Figure 1. Relation of subscale intertank to proposed RLV concepts

The intertank is 77" (1.85 m) high with IM7/8552 graphite/epoxy face sheets and a 5052 aluminum honeycomb core. The design load is 4000 lb/in ( $7 \times 10^5$  N/m) with a 1.2 peaking factor (to account for uneven loads), and safety factors of 1.4 in the acreage and 2.0 at the joints. The 8 panels were made by an Automated Tape Laying machine and oven cured. The panels were then bonded together using composite splices and a room temperature cure epoxy. At the ends, the panels taper through a "dogleg" from a sandwich to a solid composite

buildup for the bolted shear fasteners. The intertank mates to the LH2 tank skirt with a composite double lap splice. The test stand interface is through aluminum angles which are bolted to a deep steel load ring. Figure 2 shows the completed

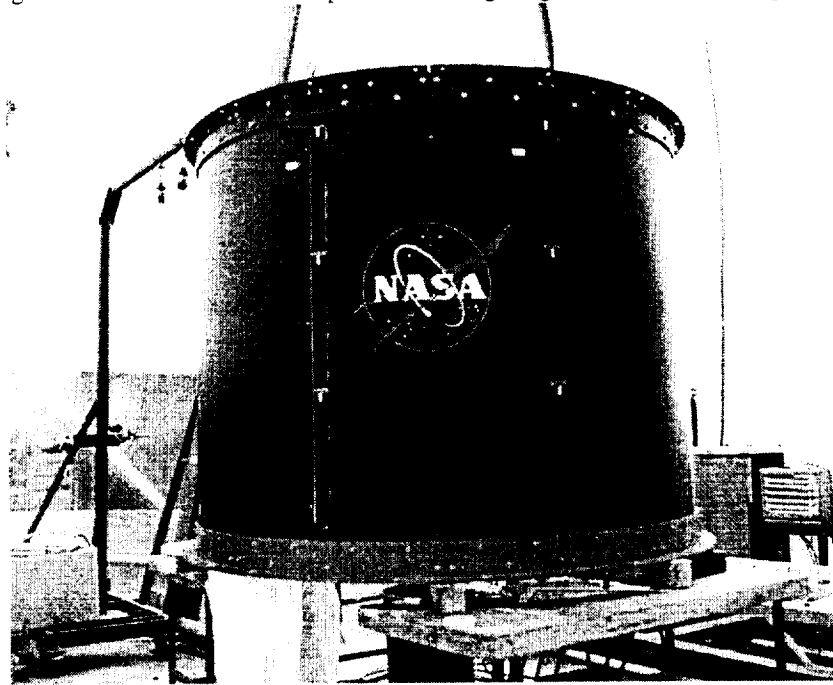


Figure 2. Composite intertank

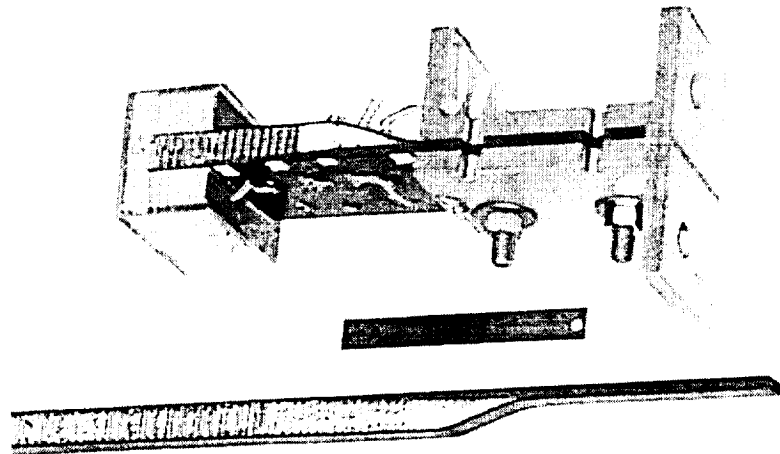


Figure 3. Dogleg configuration

intertank with the aluminum angle interfaces. Figure 3 shows a sectioned dogleg test sample and the trimmed end of one of the panels.

The initial design was performed by genetic algorithm (GA) using empirical and derived solutions for the analysis. Following the optimization, a test plan was developed in conjunction with detailed finite element modeling.

The completed intertank has undergone a 250,000 lb ( $1.1 \times 10^6$  N) limit load test and, along with the LH2 tank, is being prepared for 200 cycles of combined thermal and mechanical loading. Figure 4 shows the mated tank and intertank in the test stand. The LH2 tank is on the bottom of the stack and is wrapped in white insulation. After the cyclic loading of the system, the intertank will be removed and loaded to failure in compression.

### Optimizer analysis

The optimization program is called CHOGA for Composite Honeycomb Optimization by Genetic Algorithm. The GA was selected for its ability to handle discrete design variables such as the ply orientations, and size and number of bolts. CHOGA provided a near optimum starting point for the design process and was extremely useful in a variety of trade studies. As the design matured some variables were finalized on non-optimum values for other than numeric

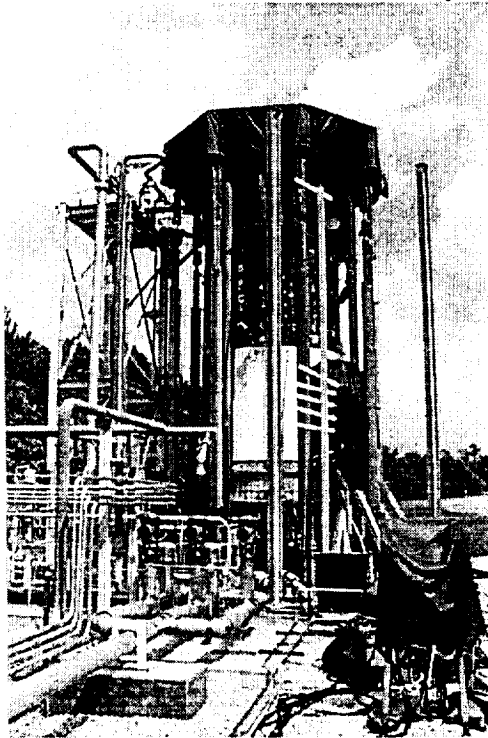


Figure 4. LH2 tank and intertank in the test stand

design considerations. CHOGA was able to accept these as input and optimize the remaining variables in the system to stay close to the optimum weight.

### Design Variables

The ply layups were coded with 4 bits to allow orientation angles of 0, 10, 15, 20, 30, 40, 45, 50, 60, 70, 75, 80, 90 degrees and "no-ply" (Smith<sup>1</sup>). The no-ply selection allows the optimizer to remove plies and optimize the number of plies as well as their orientation. After selecting the ply orientations, the layup is made symmetric and balanced, meaning the total layup may be up to four times thicker than the number of ply orientation design variables. One bit determines if plies are balanced in sequence (e.g. 10/30/20/-10/-30/-20) or by

alternating (10/-10/30/-30/20/-20). One bit is used to determine if 0° and 90° plies are copied where an angle ply would be balanced (30/-30/0/20/-20 vs. 30/-30/0/0/20/-20). Lastly, one bit determines if a center ply of 0 or 90 degrees will be made symmetric about the ply centerline, creating an odd number of plies, or by adding another ply. As an aid to design during the downselect process, layups for either the facesheets or the buildups can be input as a separate text file and removed from the chromosome.

The bolts are selected from a table of mass, diameter and shear strength. The table is a separate file and the user controls the number of bits used to select the bolt. This was useful because once the bolt size was determined the number of chromosome bits could be reduced. The optimizer preferred many small bolts which would eventually approximate an evenly distributed line load. The final design diverged from the optimum for the non-numeric reasons of time for assembly and the testing sequence. The intertank would be loaded in 3 different configurations but needed match drilled fasteners at each step to transfer shear loads. To do this, the fastener size increases for each load case. The limit load test, with the steel load ring, used 3/8" (10 mm) fasteners. The cyclic load test, mated with the composite LH2 tank, uses 7/16" (11 mm) fasteners. When loaded to failure, again with the steel load ring, 1/2" (13 mm) fasteners will be used.

The remaining design variables: core thickness, bolt edge distance and number of bolts, are given maximum and minimum values and the number of bits to use. By careful selection of these parameters an integer number of bolts is guaranteed. The number of bolts can even be controlled to multiples of 8 to account for the 8 panels of the assembly.

### Constraints

The cylinder is constrained by general buckling. The faces are constrained by strength, dimpling and wrinkling. The bolted joints are constrained by local bearing, net tension, wedge splitting, shear out, tension/shear out and bolt stress. Violations of constraints are handled by the penalty function:  $P1 * [(applied/allowable - 1) + P2]$ , where P1 and P2 are user supplied values. By including the step of P2 when a constraint is violated by even a very small amount it is possible to separate valid designs from slightly violated designs which might otherwise have an extremely small penalty. P1 \* P2 should be on the order of 0.5 to 5% of the final expected weight of the part. Typical values used in the design of the intertank were 150 for P1 and .01 for P2 for a 250 lb (1112 N) total weight.

Laminate properties for both the faces and buildups are calculated by classical lamination theory (Jones<sup>2</sup>). The secant method is used to find the allowable strengths for the laminates based on the Tsai-Hill stress criterion. Normal and shear stresses on the faces are checked. Wrinkling, the skin pushing into or pulling away from the core, and dimpling, localized skin buckling within a single cell, are also constrained on the faces (HEXCEL<sup>3</sup>).

The buckling analysis is for an orthotropic laminated cylinder (NASA<sup>4</sup>)

and iterates on the combination of axial and circumferential buckling waves until a minimum energy buckling load is found. A knockdown factor, based on empirical studies, is then applied to provide the critical buckling load.

The capacity of the buildup to carry bolt loads was based on a simplified set of equations (Chamis<sup>5</sup>). The bearing stress equation was found to be non-conservative based on coupon tests. The coupon tests were performed with no clamping force on the faces, which would have increased the bearing load. Another program, the Bolted Joint Stress Field Model (Ogonowski<sup>6</sup>) (BJSFM), correlated well with the coupon tests and was slightly conservative. BJSFM was not incorporated into the optimizer due to its application late in the design and the ability of the optimizer to accept layups as fixed input.

To keep the optimization analysis as simple as possible, the details of the dogleg were neglected. There were two reasons for this. First, early in the design cycle the tapered joint was considered most likely but a variety of alternate joints were under consideration. Therefore it was not an efficient use of time to put a detailed analysis into the program. Second, since the dogleg area is relatively small compared to the size of the entire intertank, even major changes would not significantly affect the objective function of weight.

## **Finite Element Modeling and Component Testing**

The finite element models addressed a variety of failure modes: shell buckling, stress in the face sheet skins, stress in the panel splices, the splice bondlines, crushing of the honeycomb core, and shear in both the L and W directions of the honeycomb. All laminate stresses used the Tsai-wu failure criterion. In order to calculate these margins 3 major cylinder models, 1 detailed joint model, and over 11 smaller coupon finite element models were required.

As part of the development program, a series of coupon tests were conducted and compared with finite element models. Table 1 is a list of the component tests along with the actual and predicted failure loads. Not included are the bearing tests which were not analyzed by finite elements.

Important information was derived from these tests. Tests 1, 3, 5, 11, 13 and 15 led to applying a factor of 80% to first ply failure calculations to account for any localized honeycomb shear failures. Test 7 showed that out-of-plane loads failed honeycomb at the splices causing the specimens to become non-linear before the predicted failure. This led to bonding the core together at the panel splices. Tests 9 and 21 provided model validation. Test 17 validated the use of strain energy density for the stress state in the bondline. Test 19 showed that care must be taken with the directional properties and calculations of the honeycomb since a hoop honeycomb failure would be catastrophic.

The initial model consisted of a single panel (45 degree cylinder segment) with symmetry boundary conditions. It has shell elements, 10095 degrees of freedom, and 16 separate property groups. The first buckling mode of this model is shown in Figure 5.

Table 1. Coupon/Component Tests

ID	Description	Predicted Failure	Actual Failure	Actual Predicted
1	Honeycomb sandwich, 7 ply skins, in-plane axial compression	13.47 kip	11.8 kip	88%
3	Honeycomb sandwich, 4 ply skins, in-plane axial compression	3.115 kip	3.298 kip	105%
5	Honeycomb sandwich, 14 ply skins, in-plane axial compression	27.16 kip	-	-
7	Sandwich with shear splice, out-of-plane 4-point bend	711 lb	704 lb	99%
9	Sandwich, out-of-plane 4-point bend with splices in shear region	741 lb	746 lb	100%
11	Sandwich with shear splice, in-plane 3-point bend	1265 lb	1194 lb	94%
13	Sandwich, in-plane 3-point bend	905 lb	805 lb	89%
15	Sandwich with splice, in-plane axial compression	9.48 kip	9.375 kip	99%
17	Sandwich with splice, in-plane axial tension	4.9 kip	4.98 kip	101%
19	Sandwich with 7 ply skins, in-plane transverse compression	9.2 kip	9.24 kip	100%
21	Sandwich with 7 ply skins, in-plane transverse tension	6.2 kip	6.3 kip	101%
23	Same as Test ID 1 with damage		9.01 kip	
25	Same as Test ID 19 with damage		-	
	End joint configuration, axial compression	6353 lb/in	6738 lb/in	106%

Results from the component tests indicated that the honeycomb core failed at consistently lower loads than the composite skins. This demanded a model using 3D brick elements for the honeycomb and shell elements for the skins. This 3D model was further varied by including or neglecting the offsets of the skin. The skins were either located accurately using offsets, or not offset such that the centerline of each face was modeled as being located at the surface of the core. The model with offsets was more conservative for displacements and stresses in the honeycomb, bondline and splice laminates. The model without offsets was more conservative for stresses from the end constraints. The 3D element model is shown in Figure 6.

The 3D model also had to be incorporated into different models to accurately represent the end conditions for different loadings. During limit load testing the intertank used load rings on both ends. The load rings are deep steel rings bolted to aluminum angles which interfaced to the intertank through shear

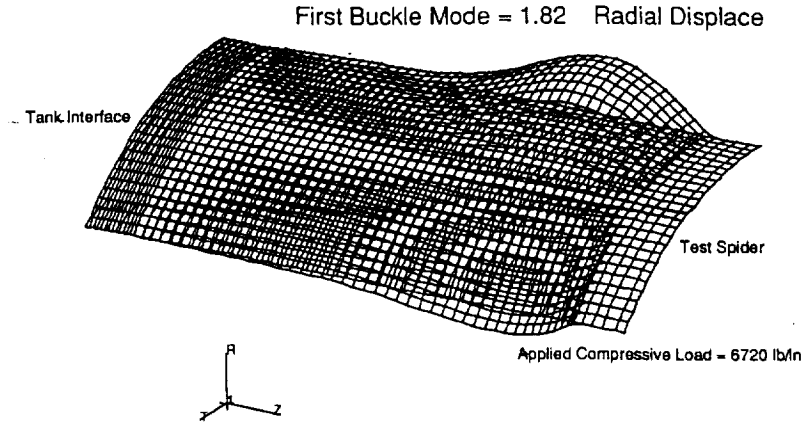


Figure 5. First buckling mode of shell element model

fasteners. For tank/intertank testing one load ring is removed and replaced with the composite LH2 tank using a bolted, double lap composite splice joint. Figure 7 shows the first buckling mode of the intertank panel mated with the LH2 tank.

The load paths and stress states in the joint, or "dogleg" region where the panels taper from the core to the bolt buildup are very complex. A high fidelity model was made of one small segment of the cylinder to study this region. This model was directly correlated with compression tests of doglegs taken from the first panel. Based on the models, a higher density core was used in the taper region to help transfer shear stresses between the skins. Also, the core was potted from the tip of the taper to just past the "knee" of the dogleg to give a larger bond to help carry locally induced tensile loads normal to the skin. Figure 8 shows the deformed results of the dogleg model.

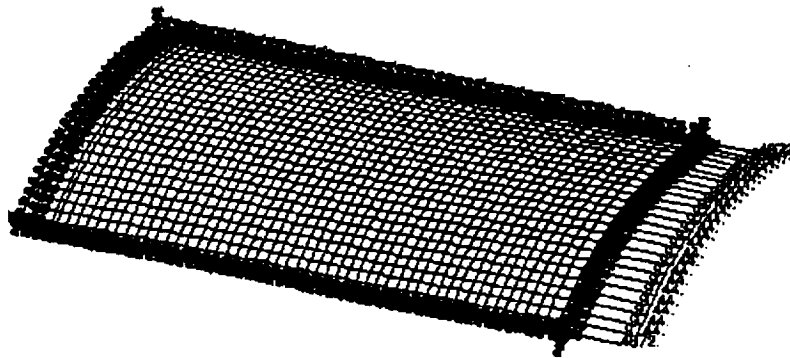


Figure 6. Finite element model using 3D bricks for the honeycomb core

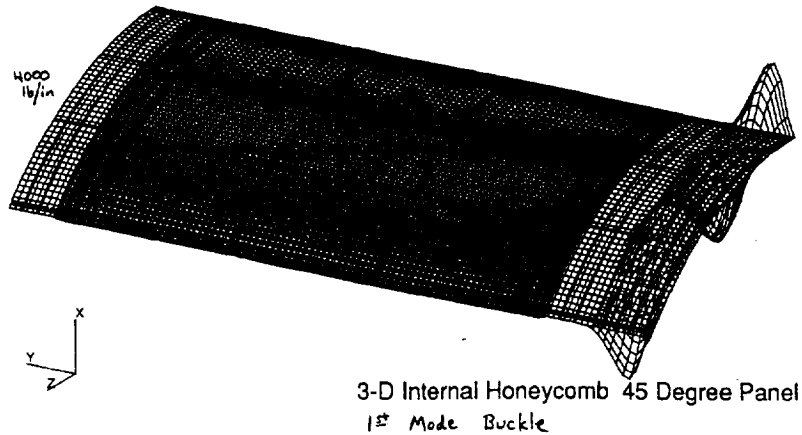


Figure 7. First buckling mode of the tank/intertank interface

### Changes from initial optimization

There were several notable changes that were required to the results from CHOGA. The core thickness had to be increased from by 0.05" (1.3 mm) to increase the buckling margin of the intertank. This change was based on the finite element analysis and was related to different values for the knockdown factor used by the optimizer and the stress analyst. The dogleg region, which was not carefully modeled in CHOGA, had to have a higher strength core over the last several inches to help transfer shear loads between skins. Potting compound was also required at the knee of the dogleg to provide a larger bonding area to react the normal tensile loads induced in the skin by the geometry of the joint. The dogleg changes were based on the finite element analysis which was verified by component test. Finally, the layup in the bolt buildup region went from 38 to 52 plies to account for bolt bearing strength. This change was based on coupon tests.

### Conclusions

The use of the GA and traditional analysis in CHOGA allowed the creation of a design tool which provided both a near optimum starting point for the design process as well as being versatile enough to incorporate enforced changes as the design matured without severely impacting the final weight. CHOGA was also useful in performing trade studies by allowing many configurations to be run overnight. The curves generated were used to quantify losses due to departing from the optimum design variables and allow informed design decisions.

Less computationally intensive analysis opens up the possibility of using

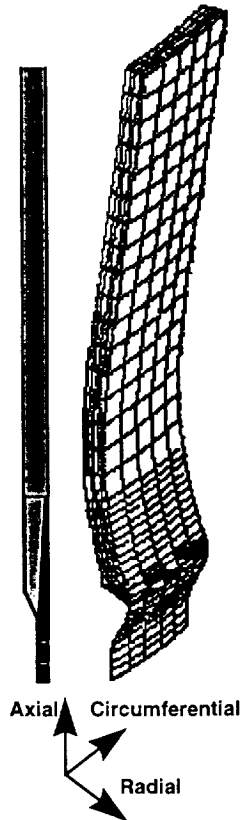


Figure 8. Deformed dogleg model

optimization tools such as the GA. The GA requires more analysis but is an ideal choice for laminate (and other integer) optimization and provides a greater confidence of avoiding local minima.

Finite element models combined with optimization codes are extremely powerful tools, but would have been difficult to apply to this design. The ply layup, a major part of the optimization, would have been difficult to address. The multiple models required would have multiplied the computing time of an already very time consuming analysis. The early configuration changes required a tool that could quickly be adapted to the requirements. Finally, the uncertainty of the correlation between analysis and reality would have prevented a useful FEM based tool from being used until very late in the design cycle.

There are many tools and many needs in structural optimization. It is important to use the right tool for the right need or the benefits of optimization, namely better products in less time, will be lost.

1. Smith, R.E., Correspondence with, University of Alabama, Department of Aerospace Engineering and Mechanics, Tuscaloosa Alabama, 1994
2. Jones, R.M., Mechanics of Composite Materials, Hemisphere Publishing Corporation, New York, 1975
3. "Bonded Honeycomb Sandwich Construction", HEXCEL TSB124, 1993
4. "Buckling of Thin-Walled Circular Cylinders," NASA SP-8007, NASA Space Vehicle Design Criteria (Structures), 1968.
5. Chamis, C.C., "Simplified Procedures for Designing Composite Bolted Joints", NASA Technical Memorandum 100281, 1988.
6. Ogonowski, J.M., "Effect of Variances and Manufacturing Tolerances on the Design Strength and Life of Mechanically Fastened Composite Joints, Volume 3 - Bolted Joint Stress Field Model (BJSFM) Computer Program User's Manual", AFWAL-TR-81-3041, Vol 3, Wright-Patterson Air Force Base, 1981